Research Paper

Comprehensive characterization of AP-1 adaptor complex genes in lung cancer reveals AP1AR as a novel prognostic and therapeutic biomarker

Dahlak Daniel Solomon[1,2#], I-Jeng Yeh[3,4#], Hsin-Liang Liu[3], Che-Yu Su[3], Yung-Kuo Lee[5,6,7], Ching-Chung Ko[8,9,10], Hui-Ru Lin[7,11], Sachin Kumar[1,12,13], Do Thi Minh Xuan[14], Neethu Palekkode[1,15], Ayman Fathima[1,16], Hung-Yun Lin[1,17,18,19,20], Chih-Yang Wang[1,12,17✉], Meng-Chi Yen[3,4✉]

1. Graduate Institute of Cancer Biology and Drug Discovery, College of Medical Science and Technology, Taipei Medical University, Taipei 11031, Taiwan.
2. Yogananda School of AI Computers and Data Sciences, Shoolini University, Solan 173229, India.
3. Department of Emergency Medicine, Kaohsiung Medical University Hospital, Kaohsiung Medical University, Kaohsiung 80708, Taiwan.
4. Graduate Institute of Clinical Medicine, College of Medicine, Kaohsiung Medical University, Kaohsiung 80708, Taiwan.
5. Medical Laboratory, Medical Education and Research Center, Kaohsiung Armed Forces General Hospital, Kaohsiung 80284, Taiwan.
6. Division of Experimental Surgery Center, Department of Surgery, Tri-Service General Hospital, National Defense Medical University, Taipei, 11490, Taiwan.
7. Institute of Medical Science and Technology, National Sun Yat-Sen University, Kaohsiung, 80424, Taiwan.
8. Department of Medical Imaging, Chi-Mei Medical Center, Tainan, Taiwan.
9. Department of Health and Nutrition, Chia Nan University of Pharmacy and Science, Tainan, Taiwan.
10. School of Medicine, College of Medicine, National Sun Yat-Sen University, Kaohsiung, Taiwan.
11. Nursing Department, Kaohsiung Armed Forces General Hospital, Kaohsiung 80284, Taiwan.
12. Ph.D. Program for Cancer Molecular Biology and Drug Discovery, College of Medical Science, Taipei Medical University, Taipei 11031, Taiwan.
13. Faculty of Applied Sciences and Biotechnology, Shoolini University of Biotechnology and Management Sciences, Himachal Pradesh, India.
14. Faculty of Pharmacy, Van Lang University, 69/68 Dang Thuy Tram Street, Binh Loi Trung Ward, Ho Chi Minh City, 70000, Vietnam.
15. Department of Biotechnology, Mother Teresa Women's University, Kodaikanal, Tamil Nadu, 624101, India.
16. Computer Engineering with specialization in Artificial Intelligence and Machine Learning, Presidency University, Yelahanka, Bengaluru 560064 India.
17. TMU Research Center of Cancer Translational Medicine, Taipei Medical University, Taipei 11031, Taiwan.
18. Traditional Herbal Medicine Research Center of Taipei Medical University Hospital, Taipei Medical University, Taipei 11031, Taiwan.
19. Cancer Center, Wan Fang Hospital, Taipei Medical University, Taipei 11031, Taiwan.
20. Pharmaceutical Research Institute, Albany College of Pharmacy and Health Sciences, Rensselaer, NY 12144, USA.

# Equal contributors.

✉ Corresponding authors: Chih-Yang Wang (chihyang@tmu.edu.tw) and Meng-Chi Yen (yohoco@gmail.com).

Abstract

Lung cancer remains the leading cause of cancer mortality. The AP-1 adaptor complex, including AP1AR, AP1S1, AP1S2, AP1S3, AP1M1, AP1M2, AP1B1, and AP1G1, functions as a conserved hub of vesicular trafficking, selecting cargo and coordinating clathrin-mediated transport. By shaping receptor recycling, membrane composition, and signal duration, AP-1 influences core cancer phenotypes such as proliferation, migration, and therapy response. However, the family-level role of AP-1 adaptors in lung cancer is incompletely defined. We systematically profiled all eight AP-1 adaptor genes using multi-omics datasets, survival resources, pharmacogenomic panels, Human Protein Atlas data, pathway enrichment, and single-cell RNA sequencing with cell–cell communication modeling. *AP1AR* was consistently upregulated in lung adenocarcinoma and independently associated with poorer overall survival. It was linked to cell-cycle progression, DNA replication checkpoints, hypoxia, and epithelial-to-mesenchymal transition (EMT). At single cell resolution, *AP1AR* also regulate malignant epithelial and fibroblast cell types. Pseudotime analyses revealed progressive activation along proliferative and EMT axes, and CellChat modeling indicated enhanced stromal and epithelial signaling. *AP1S3* and *AP1S1* showed complementary roles, associated with oncogenic/inflammatory signaling and immune-metabolic programs, respectively. These findings identify *AP1AR* as a clinically relevant biomarker and highlight AP-1 adaptor biology as an underexplored contributor to lung adenocarcinoma progression and therapeutic stratification.

Keywords: AP-1 adaptor complex, AP1AR, lung cancer, biomarker, multi-omics analysis, single-cell RNA sequencing, prognosis and therapeutic target

1. Introduction

Lung cancer remains the leading cause of cancer-related mortality worldwide, with survival rates remaining poor despite advances in molecularly targeted therapies and immunotherapy [1, 2]. Identifying novel molecular regulators of tumor progression is therefore essential for discovering new biomarkers and therapeutic targets [3-5]. Non-small-cell lung cancer (NSCLC) accounts for approximately 85% of cases and is primarily divided into two major histological subtypes: lung adenocarcinoma (LUAD) and lung squamous cell carcinoma (LUSC). Adaptor protein (AP) complexes are evolutionarily conserved regulators of intracellular trafficking that mediate cargo sorting among endosomes, lysosomes, and the trans-Golgi network [6]. Among them, the AP-1 adaptor complex plays a central role in clathrin-mediated transport, linking membrane dynamics to cell signaling and homeostasis [7]. Dysregulation of AP complexes has been implicated in several cancers, where altered vesicle trafficking can affect oncogenic receptor turnover, nutrient signaling, and immune evasion [8-10]. While several AP-1 adaptor subunits, such as *AP1B1* and *AP1G1*, have been studied in cancer [11, 12], a systematic evaluation of the AP-1 adaptor family in lung cancer is lacking. Notably, AP1AR (adaptor protein complex 1-associated regulatory) has not been characterized in lung cancer or other solid tumors, representing an opportunity to explore novel mechanisms of tumor regulation.

Recent multi-omics resources enable comprehensive evaluation of gene families across diverse cancer datasets [13-17]. Integrative analyses combining bulk transcriptomics, clinical outcomes, protein expression, drug-sensitivity correlations, pathway enrichment, and single-cell data allow robust characterization of candidate genes [18-20]. Using this approach, we present the first systematic analysis of eight AP-1 adaptor genes in lung cancer. We show that *AP1AR* is consistently upregulated, associated with poor survival, enriched for cell-cycle and epithelial-to-mesenchymal transition (EMT) pathways, and localized to malignant epithelial and fibroblast cell types at the single-cell level. *AP1S3* and *AP1S1* provide complementary support, while other family members offer broader context. These findings establish *AP1AR* as a novel prognostic biomarker and potential therapeutic target and highlight the AP-1 adaptor complex as an underexplored contributor to lung cancer biology.

2. Materials and Methods

2.1 RNA-seq Expression and Clinical Data

Transcriptomic expression data and corresponding clinical annotations for LUAD and normal lung tissues were obtained from UALCAN, which compiles The Cancer Genome Atlas (TCGA) Level 3 RNA-seq (HTSeq-FPKM) datasets [21, 22]. Analyses included tumor versus regular comparisons, pathological stage-specific profiling, and pan-cancer assessments. Expression values were log2-transformed as transcripts per million (TPM + 1) to ensure comparability across datasets. Prognostic associations were evaluated using three independent platforms to enhance reproducibility [23-25]. SurvivalGenie v2.0 was used to generate volcano plots and multivariate Cox regression-based forest plots across TCGA cohorts [26]. GEPIA2 provided Kaplan–Meier survival curves and hazard ratios, while KMplotter was employed to validate associations in independent LUAD samples [27, 28]. Patients were stratified into high- and low-expression groups based on the median value unless otherwise indicated [29-31]. Statistical significance was determined using log-rank *p* values, with hazard ratios (HRs) and 95% confidence intervals (CIs) reported.

2.2 DNA-Methylation and Protein Expression Profiling

DNA-methylation data for *AP1AR* and *AP1S3* were obtained from the TCGA-LUAD and TCGA-LUSC cohorts via the UCSC Xena browser, and promoter-level β-values were analyzed [32]. Methylation profiles were visualized using heatmaps and boxplots to compare tumor and adjacent normal tissues. Functional dependency data from DepMap (23Q4 release) were used to assess the essentiality of *AP1AR* and *AP1S3* across lung cancer cell lines [33]. Protein expression and subcellular localization were evaluated using immunohistochemistry (IHC) data from the Human Protein Atlas (HPA) [34]. Representative staining images for normal and tumor lung tissues were examined, and staining intensity was classified as not detected, low, medium, or high. Localization patterns were compared between tumor and normal specimens to validate transcriptomic observations at the protein level [35-37].

2.3 Drug-Sensitivity and Gene Set Enrichment and Pathway Analyses

Drug response correlations were analyzed through the Gene Set Cancer Analysis (GSCA) platform [38], supplemented with data from the Cancer Therapeutics Response Portal (CTRP) [39] and the Genomics of Drug Sensitivity in Cancer (GDSC) [40]. Gene expression levels were correlated with half-maximal inhibitory concentration (IC_{50}) values

using Pearson or Spearman correlation coefficients. Associations with false discovery rate (FDR)-adjusted *p* values of < 0.05 were considered statistically significant [41-43]. Functional enrichment analyses were performed using Gene Set Enrichment Analysis (GSEA) and MetaCore (Clarivate Analytics). GSEA was conducted utilizing the fgsea R package (Bioconductor v3.19) [44], which employs hallmark and curated gene sets from the Molecular Signatures Database (MSigDB v7.5.1) [45]. Analyses were based on 10,000 permutations, and pathways with normalized enrichment scores (NESs) and an FDR of < 0.05 were considered significant. MetaCore was used to validate enrichment results and identify curated pathways relevant to cancer progression [46-48]. Additionally, protein-protein interaction (PPI) networks among the eight AP-1 adaptor genes were generated using STRING v12.0, with a medium-confidence threshold set to 0.4 to identify functionally relevant interactions [49].

2.4 Single-Cell Transcriptomic and Cell-Cell Communication Analysis

Single-cell RNA-seq data were analyzed using the GSE202159 dataset [50], accessed via the cellxgene platform [51]. Processed data, including quality-controlled cell clusters and annotated major lineages (epithelial, fibroblast, endothelial, myeloid, lymphoid, and T/natural killer (NK) cells), were used for downstream analyses. Gene expression patterns of the AP-1 adaptor genes were visualized using t-distributed stochastic neighbor embedding (t-SNE) dimensionality-reduction techniques. Expression intensities were displayed on feature plots, and relative enrichment was assessed across clusters via heatmaps [52-54]. Cell-cycle states (G1, S, and G2/M) were inferred using canonical phase markers. Pseudotime trajectories were reconstructed using the Slingshot algorithm within the SingleCellPipeline (SCP) package to infer lineage relationships and temporal expression trends for *AP1AR* and *AP1S3*. Correlation analyses were performed against DNA-repair gene sets (*BRCA1*, *RAD51*, *ATM* and *PARP1)*. Clinical metadata, including tumor stage, histological subtype, and smoking status, were integrated for contextual interpretation and analysis [55-58]. Clinical metadata, including tumor stage, histological subtype, and smoking status, were incorporated to contextualize expression patterns within tumor progression. To evaluate intercellular signaling networks associated with target gene expressions, CellChat [59] was applied to the GSE202159 object. Separate analyses were performed for high- and low-expression cell subsets. The inferred signaling probabilities were visualized as global communication networks, lineage-specific connectivity heatmaps, and directional sender-receiver maps [60-64].

2.5 Statistical Analysis

All analyses were performed using publicly available platforms and locally installed software [65-67]. Data handling and visualization used R/RStudio with the ggplot2 package [68-70], SPSS (IBM, Armonk, NY, USA) [71]. Additional exploratory analyses were conducted with Omics Playground v3.4.1[72] and SRPlot [73-75]. Quantitative data are reported as mean ± standard deviation (SD) from at least three independent experiments [73-75]. Group differences were assessed using one-way or two-way analyses of variance (ANOVA), followed by Bonferroni correction for multiple comparisons [76, 77]. Survival analyses were performed using the Kaplan–Meier method and compared with the log-rank test [78-80]. HRs with corresponding 95% CIs were estimated using Cox proportional hazards models when appropriate. Unless otherwise indicated, statistical tests were two-sided, and a *p* value < 0.05 was considered statistically significant.

3. Results

3.1 Expression and Prognostic Relevance Extents of *AP-1* Adaptor Genes in Lung Cancer

A systematic multi-omics analysis was conducted for the eight AP-1 adaptor complex genes (*AP1AR, AP1B1, AP1G1, AP1G2, AP1M1, AP1M2, AP1S1,* and *AP1S3*) to characterize their roles in lung cancer. These genes were investigated by integrating bulk RNA-seq, clinical outcomes, protein expression, drug-sensitivity correlations, pathway enrichment, and single-cell transcriptomics. To identify key candidates, gene expression patterns and associations with patient survival were first evaluated across TCGA datasets using the UALCAN platform. Among the eight genes, *AP1AR*, *AP1S1*, and *AP1S3* were consistently upregulated in LUAD relative to normal lung tissues (Figure 1A, C, E), whereas other family members showed variable or minimal changes (Supplementary Figure S1). Kaplan–Meier analyses indicated that high expression of *AP1AR* and *AP1S3* correlated with shorter overall survival (OS), with *AP1S1* showing a weaker but similar trend (Figure 1B, D, F). Multivariate Cox regression using SurvivalGenie confirmed *AP1AR* and *AP1S3* as independent adverse prognostic markers (HRs > 1, *p* < 0.05), while *AP1S1* did not reach statistical significance (Figure 2A). Pathological stage-specific analyses revealed progressive upregulation of *AP1AR* and *AP1S3* with advancing tumor stage, whereas

AP1S1 expression remained relatively stable (Figure 2B–E). Kaplan–Meier survival curves further confirmed that high expression of *AP1AR*, *AP1S1*, and *AP1S3* was associated with reduced OS, with *AP1AR* and *AP1S3* showing the strongest effects (Figure 2F–H). A forest plot integrating HRs across cohorts validated *AP1AR* and *AP1S3* as independent adverse prognostic markers (Figure 2I), whereas *AP1M2* and *AP1B1* showed modest survival effects (Supplementary Figure S2). Extended analyses in TCGA-LUSC and combined TCGA-LUAD_LUSC cohorts confirmed the LUAD-specific prognostic relevance of *AP1AR* and *AP1S3* (Supplementary

Figure S3A–B). DepMap gene-effect profiles indicated moderate dependency of LUAD cell lines on these genes, supporting their role in tumor viability (Supplementary Figure S3C). Integration with TCGA methylation data revealed consistent promoter hypomethylation for *AP1AR* and *AP1S3* in LUAD (Supplementary Figure S4A–C), correlating with elevated transcript levels. LUSC analyses showed weaker but directionally consistent trends (Supplementary Figure S4D–F), suggesting that transcriptional activation of these genes is at least partly epigenetically regulated.
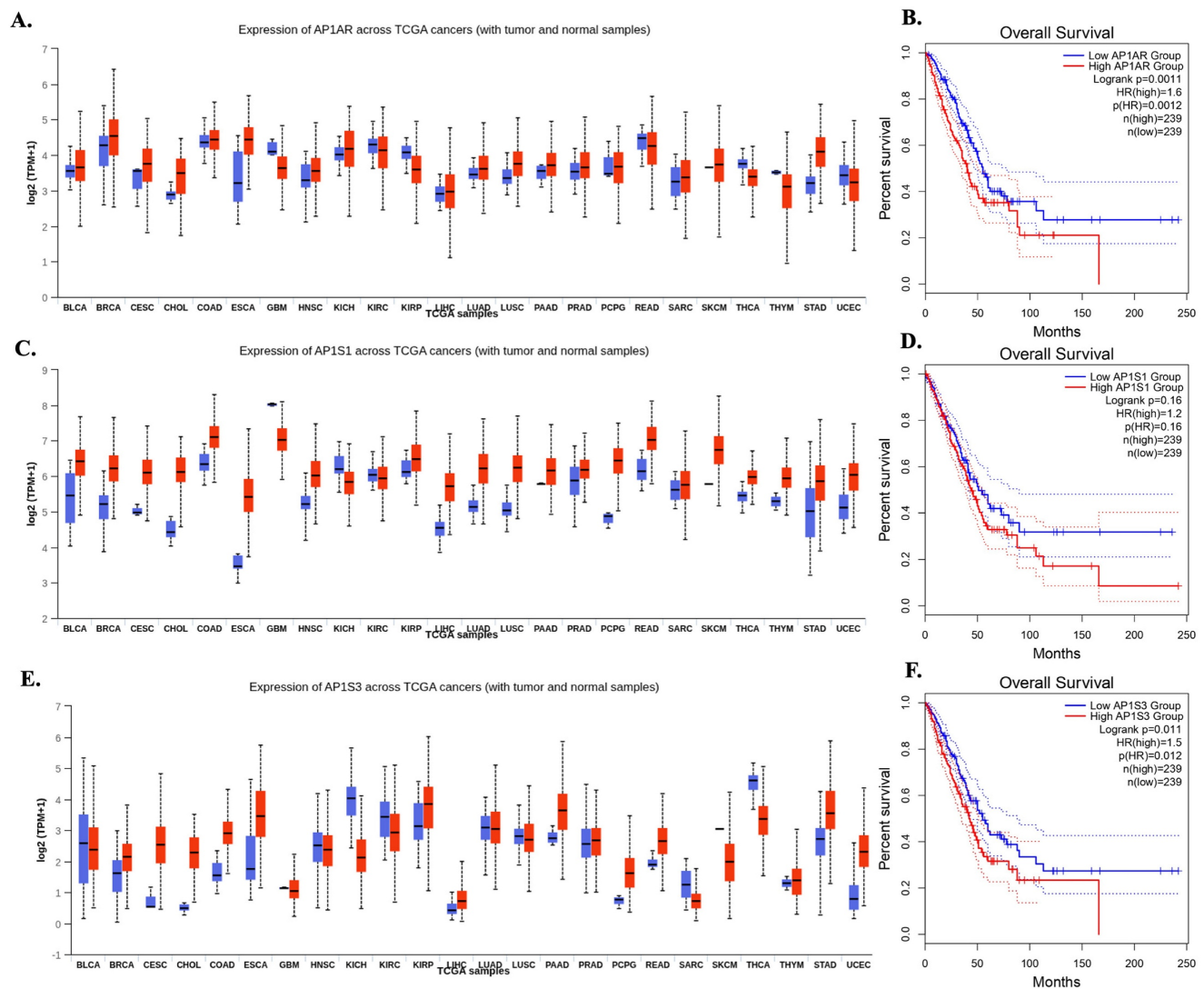
Figure 1. Pan-cancer expression and overall survival associations of AP-1 adaptor genes. (A, C, E) Boxplots showing expression of *AP1AR* (A), *AP1S1* (C), and *AP1S3* (E) across TCGA cancer types, comparing tumor (red) and normal (blue) samples. Expression is shown in log2 TPM+1. Cancer types are indicated on the x-axis. **(B, D, F)** Kaplan-Meier overall survival curves for high vs low expression of *AP1AR* (B), *AP1S1* (D), and *AP1S3* (F). Log-rank p values, Cox hazard ratios (HRs), and the number of patients in each group are indicated in the plots.
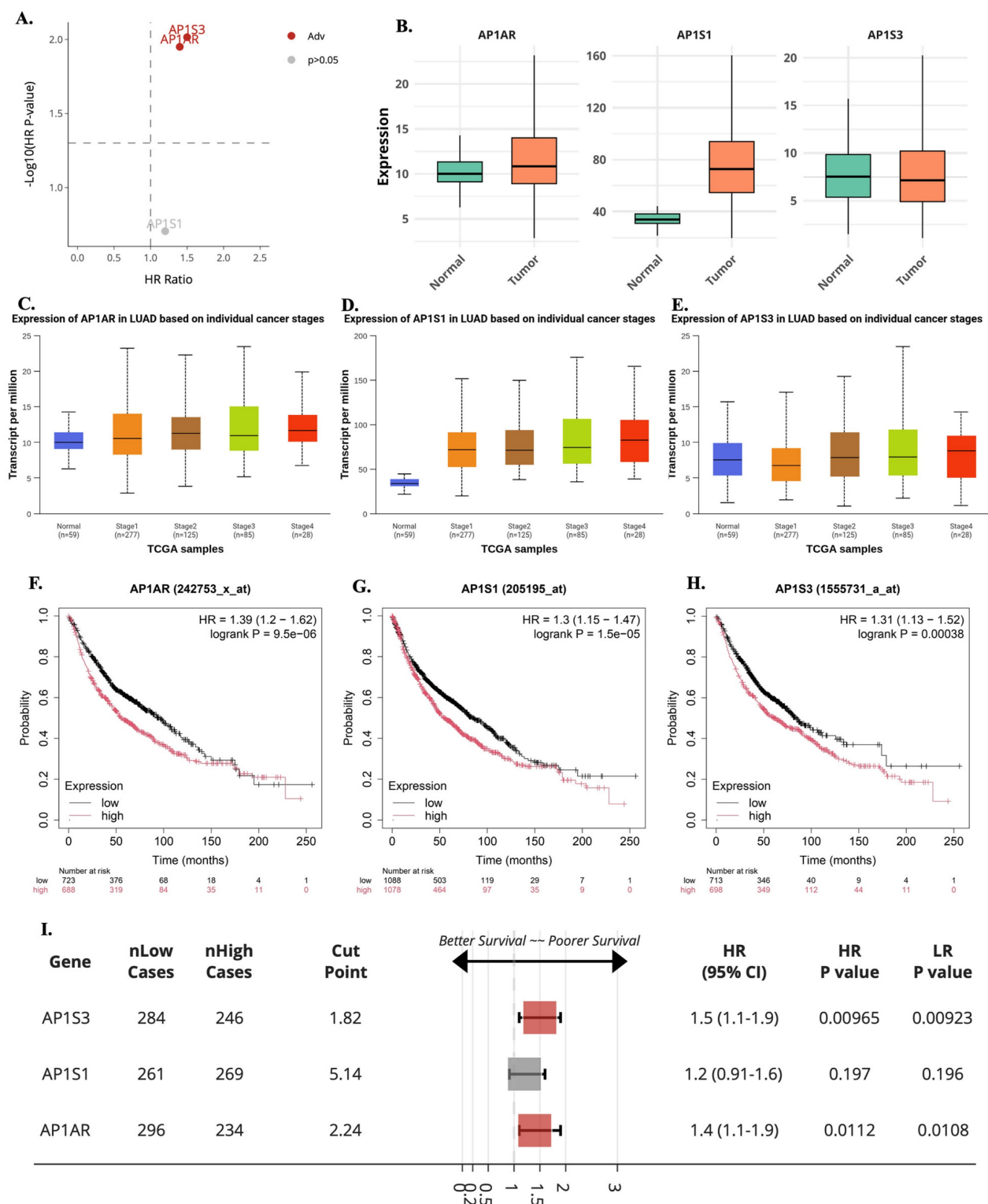
Figure 2. Expression, stage distribution, and survival associations of *AP1AR*, *AP1S1*, and *AP1S3* in lung adenocarcinoma (LUAD). (A) Multivariate Cox regression-based volcano plot from the SurvivalGenie platform highlighting *AP1S3* and *AP1AR* as adverse prognostic genes (HR > 1, *p* < 0.05). Gray dots indicate non-significant genes (*p* > 0.05). **(B)** Boxplots comparing *AP1AR, AP1S1*, and *AP1S3* expression between normal and LUAD tumor tissues. **(C–E)** Stage-specific expression patterns for *AP1AR* (C), *AP1S1* (D), and *AP1S3* (E), showing progressive upregulation of *AP1AR* and *AP1S3* with advancing tumor stage, while *AP1S1* remained relatively stable. **(F–H)** Kaplan–Meier overall survival curves for *AP1AR* (F), *AP1S1* (G), and *AP1S3* (H), indicating that high expression correlates with poorer survival, with *AP1AR* and *AP1S3* showing the strongest effects. **(I)** Forest plot summarizing hazard ratios (HRs) and 95% confidence intervals across datasets for *AP1S3, AP1S1* and *AP1AR*, confirming *AP1AR* and *AP1S3* as independent adverse prognostic markers in LUAD.

3.2 Functional Pathway Enrichment of *AP1AR*, *AP1S1*, and *AP1S3*

To explore the biological roles of the most relevant AP-1 adaptor genes, we performed GSEA on TCGA-LUAD expression profiles. *AP1AR* was strongly enriched in pathways related to EMT, hypoxia, inflammatory response, and cell-cycle progression, highlighting its role in proliferation and tumor aggressiveness (Figure 3A, D). *AP1S1* showed enrichment for IL6-JAK-STAT3 and TNFα-NFκB signaling, as well as apoptosis and G2/M checkpoint pathways, suggesting involvement in both metabolic regulation and tumor-immune interactions (Figure 3B, E). *AP1S3* was enriched in oxidative phosphorylation, fatty acid metabolism, and cell-cycle checkpoint control, indicating a link to metabolic rewiring and stress adaptation (Figure 3C, F). Supplementary analyses confirmed that other AP-1 adaptor genes were also associated with hallmark cancer pathways, including hypoxia, apoptosis, metabolism, and EMT, supporting a broader oncogenic role for the family (Supplementary Figure S5). Parallel enrichment analyses in the TCGA-LUSC cohort showed similar patterns for *AP1AR* (Supplementary Figure S6A, D), *AP1S1* (Supplementary Figure S6B, E), and *AP1S3* (Supplementary Figure S6C, F), involving EMT, PI3K/AKT/mTOR, apoptosis, and G2/M checkpoint pathways. These results indicate that transcriptional programs associated with AP-1 adaptor dysregulation are largely conserved across lung cancer histotypes.

3.3 Protein-Level Validation, Drug Sensitivity Correlations, and MetaCore Analysis

To validate transcriptomic findings, protein expression of *AP1AR, AP1S1*, and *AP1S3* was assessed using IHC data from the HPA. *AP1AR* showed detectable cytoplasmic and membranous staining in LUAD tissues, whereas *AP1S1* was weakly expressed and *AP1S3* minimally detected (Figure 4A, C, E). Quantitative summaries confirmed higher protein-level prevalence of *AP1AR* compared with the other two genes (Figure 4B, D, F). Drug sensitivity correlations were analyzed using GSCA, CTRP, and GDSC datasets. Elevated *AP1AR* expression was associated with relative resistance to multiple chemotherapeutic agents and targeted inhibitors (Figure 4G, H), whereas *AP1S1* and *AP1S3* correlated with increased sensitivity to specific small-molecule drugs, indicating differential therapeutic implications among adaptor family members. Supplementary analyses revealed that *AP1M2* and *AP1B1* were also associated with drug sensitivity in select contexts (Supplementary Figure S7). To gain mechanistic

insights, MetaCore pathway analyses were performed for *AP1AR* and *AP1S3*, the two most clinically significant genes. *AP1AR* was primarily linked to cell-cycle regulation and DNA replication checkpoints, suggesting a role in sustaining tumor proliferation (Figure 5A–B). In contrast, *AP1S3* was associated with PI3K/AKT signaling and immune/inflammatory cross-talk pathways, highlighting its involvement in integrating oncogenic and microenvironmental signals (Figure 5C–D). Supplementary analyses further revealed enrichment of *AP1AR* in cytoskeletal remodeling and adhesion pathways, and *AP1S3* in extracellular matrix remodeling and adhesion pathways (Supplementary Figure S8).

## 3.4 Single-Cell Localization of AP-1 Adaptor Gene Expressions

We analyzed single-cell RNA-seq data from GSE202159 to determine the cellular distributions and transcriptional contexts of AP-1 adaptor genes. Across ~83,000 cells, *AP1AR* and *AP1S3* were predominantly expressed in malignant epithelial and fibroblast populations, with minimal detection in immune clusters (Figure 6A–C). Lineage-specific pseudotime trajectories constructed using Slingshot revealed progressive activation of *AP1AR* along epithelial and fibroblast branches, consistent with a proliferative trajectory (Figure 6D). Differential-expression mapping highlighted widespread transcriptional upregulation associated with *AP1AR*, *AP1S1*, and *AP1S3*, implicating them in proliferative and stress-response programs (Figure 6E). Cell-cycle analysis demonstrated that most *AP1AR*- and *AP1S3*-positive cells resided in S and G2/M phases, indicating enrichment within proliferative cell types (Figure 6F). Integration with clinical annotations showed higher *AP1AR* and *AP1S3* expression in advanced-stage tumors and smoker-associated samples compared to non-tumor tissues, suggesting a link to aggressive disease phenotypes (Figure 6G). Supplementary analyses confirmed these patterns: *AP1M1, AP1B1*, and *AP1G1* exhibited moderate epithelial enrichment, whereas *AP1M2* was sparsely expressed (Supplementary Figure S9). Trajectory inferences using the SCP package revealed dynamic temporal regulation of *AP1AR* and *AP1S3*. t-SNE visualizations illustrated *AP1AR* expression across metastatic, primary, and recurrent samples, with higher signals in cells annotated as S and G2/M phases (Supplementary Figure S10A, B). Correlation analyses revealed significant associations between *AP1AR* expression and DNA-repair-related genes (Supplementary Figure S10C). Pseudotime trajectories depicted progressive *AP1AR* activation along

EMT-like branches and mid-trajectory peaks for *AP1S3*, consistent with complementary roles in proliferation and stress adaptation (Supplementary Figure S10D–G).

3.5 Microenvironmental Communication Networks Associated with *AP1AR* Expression

To investigate how *AP1AR* influences tumor–stromal interactions, we performed CellChat analysis, stratifying tumors by *AP1AR* expression. The *AP1AR*-high group exhibited markedly enhanced intercellular communication within the tumor microenvironment (TME) (Figure 7). In these tumors,

fibroblast and epithelial populations acted as dominant signaling hubs, with extensive outgoing and incoming interactions involving myeloid and T/NK cells (Figure 7A–C). These interactions were enriched in growth factor- and cytokine-mediated pathways, including TGFB1–TGFBR2, IL6–IL6R, and EGF–EGFR signaling, suggesting that *AP1AR* upregulation amplifies paracrine networks supporting tumor proliferation and immune remodeling. In contrast, *AP1AR*-low tumors displayed globally reduced communication densities and weaker cross-lineage connectivity (Supplementary Figure S11), with the most pronounced loss observed in
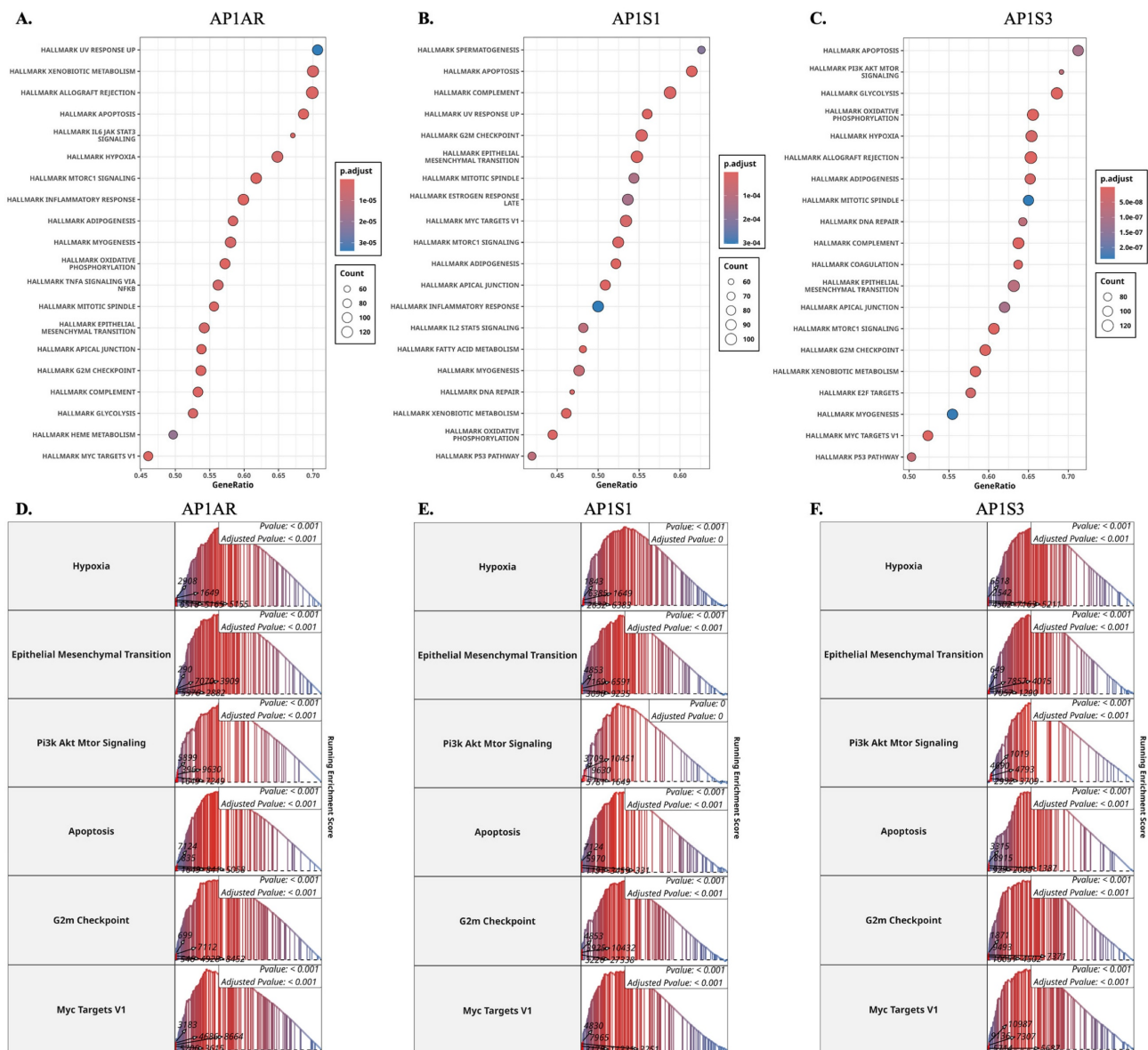

Figure 3. Gene set enrichment analysis (GSEA) of AP-1 adaptor genes in lung cancer. (A–C) Dot plots showing significantly enriched Hallmark pathways associated with *AP1AR*, *AP1S1*, and *AP1S3* expression in LUAD samples. Dot size represents gene count, and dot color indicates adjusted p-values. **(D–F)** Representative enrichment plots highlighting key Hallmark pathways, including Hypoxia, Epithelial–Mesenchymal Transition, PI3K/AKT/MTOR signaling, Apoptosis, G2M checkpoint, and MYC Targets V1 for *AP1AR*, *AP1S1*, and *AP1S3*.

fibroblast-to-epithelial and immune-to-tumor signaling. Quantitative summaries confirmed decreased pathway activity and reduced ligand–receptor diversity, highlighting *AP1AR* expression as a key determinant of intercellular signaling intensity in lung cancer. Together, these results indicate that *AP1AR* overexpression not only drives intrinsic tumor proliferation but also promotes a communication-intensive TME, characterized by epithelial–fibroblast crosstalk and immune modulation, consistent with its enrichment in EMT and cytokine-response pathways observed in GSEA results.

4. Discussion

This study represents the first comprehensive analysis of the AP-1 adaptor gene family in lung cancer, integrating bulk RNA-seq, clinical outcomes, protein expressions, drug sensitivity correlations, pathway enrichment, DNA methylation, CRISPR dependency, intercellular signaling inference, and single-cell transcriptomic data. By systematically evaluating eight AP-1 adaptor genes, we identified *AP1AR* as consistently upregulated, associated with poor survival, linked to drug resistance, and enriched in hallmark oncogenic pathways. Integration of
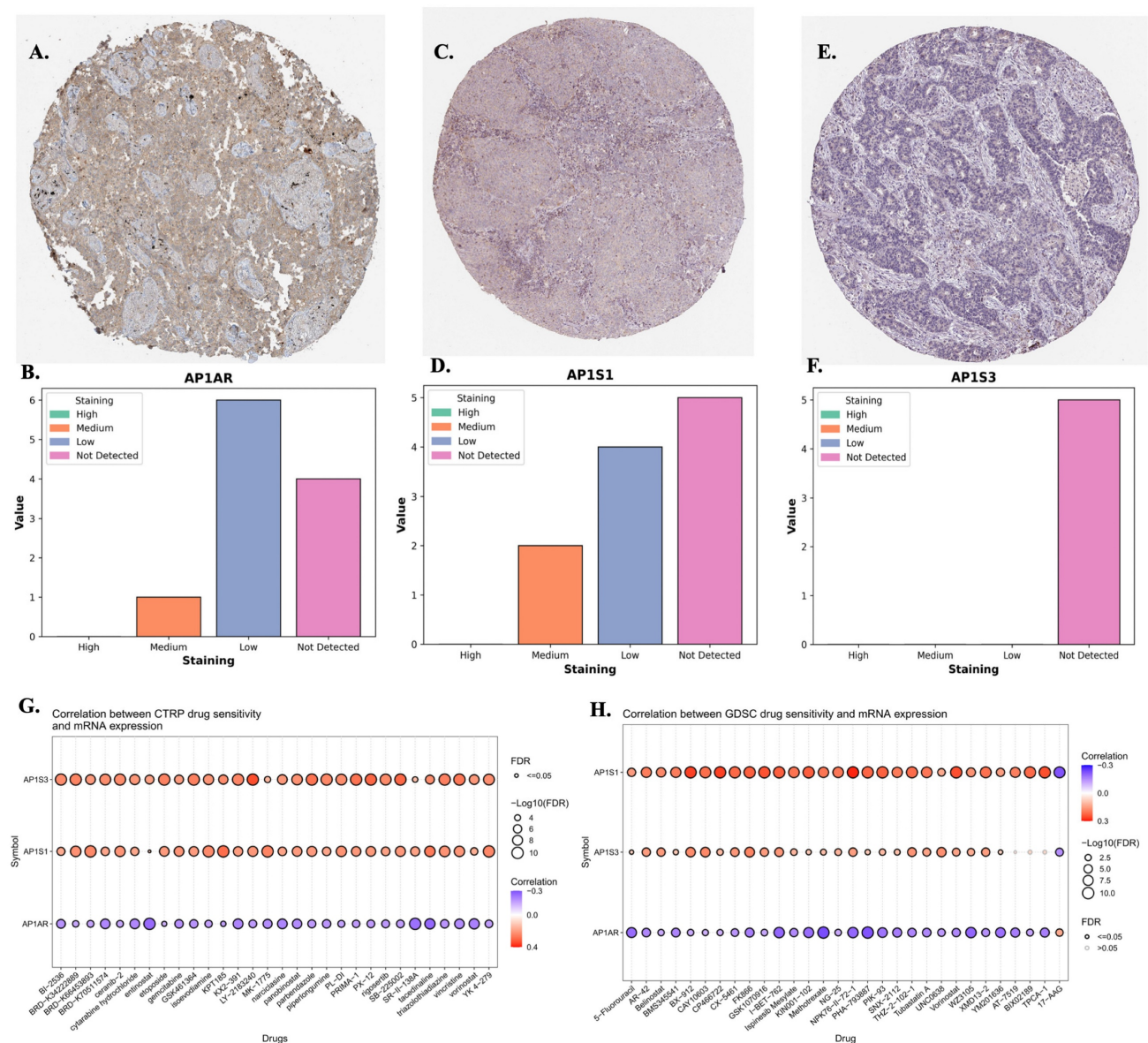

Figure 4. Protein expressions and drug-sensitivity correlations of *AP1AR*, *AP1S1*, and *AP1S3*. (A, C, E) Representative immunohistochemical (IHC) images from the Human Protein Atlas showing *AP1AR*, *AP1S1*, and *AP1S3* staining, respectively, in lung adenocarcinoma (LUAD) tissues. **(B, D, F)** Semi-quantitative distribution of staining intensities (high, medium, low, not detected) across LUAD samples, indicating that *AP1AR* is more frequently detected at the protein level than *AP1S1* and *AP1S3*. **(G)** Correlations between *AP1S3*, *AP1S1* and *AP1AR* mRNA expression and drug sensitivity in cancer cell lines from the CTRP dataset. **(H)** Correlations between *AP1S1*, *AP1S3* and *AP1AR* mRNA expression and drug sensitivity in the GDSC dataset. In (G–H), each bubble represents one drug; bubble color denotes the correlation coefficient (purple, negative; red, positive), and bubble size is proportional to −log10(FDR), with larger bubbles indicating stronger statistical significance.

promoter methylation and CRISPR dependency profiles confirmed that this transcriptional upregulation reflects both epigenetic activation and functional relevance, underscoring the biological significance of *AP1AR*. Importantly, *AP1AR* has not previously been characterized in lung cancer, highlighting its novelty and potential clinical value.
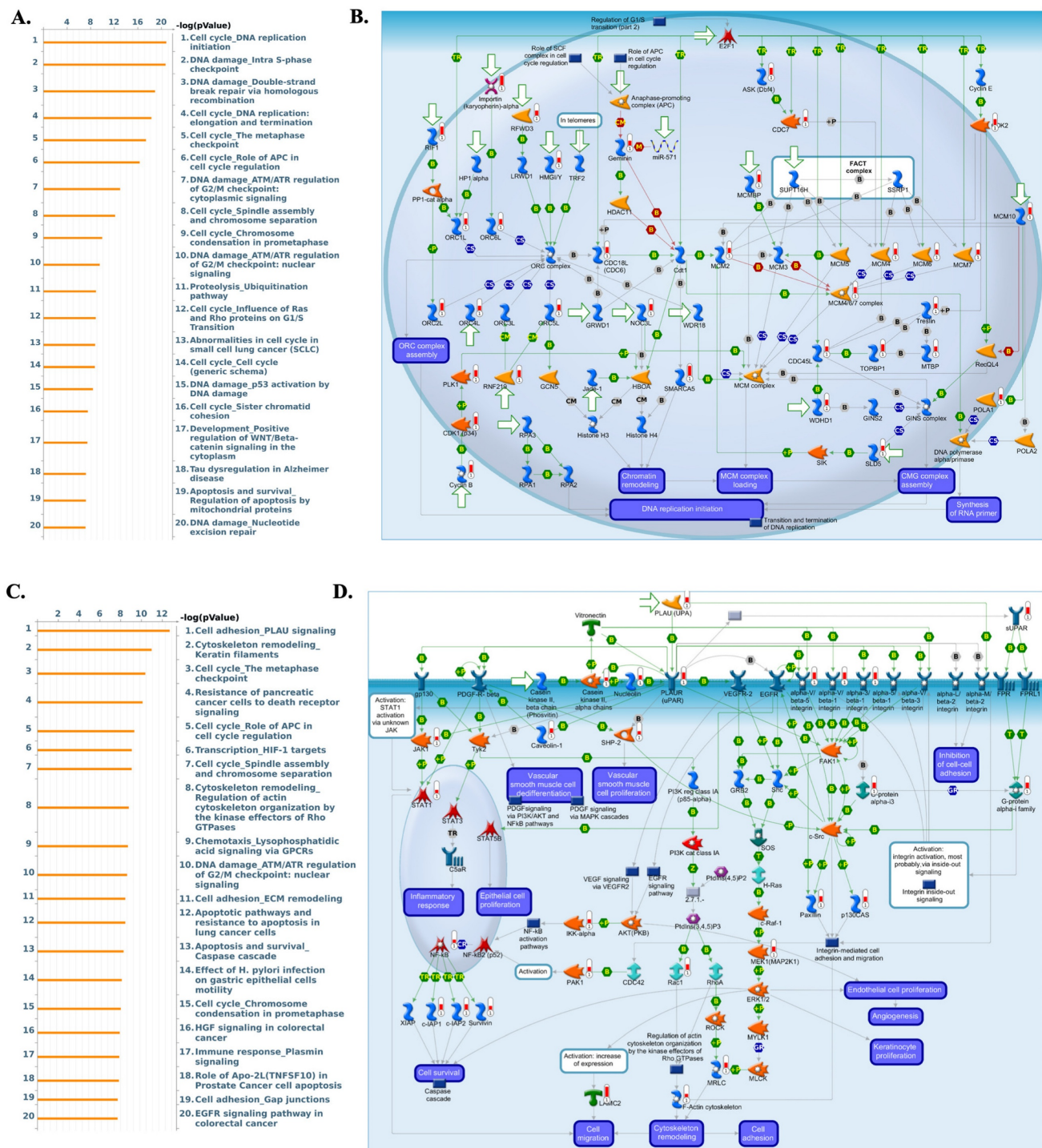
Figure 5. Pathway enrichment analysis of *AP1AR*- and *AP1S3*-associated gene signatures in lung adenocarcinoma (LUAD). (A) Bar plot of the top 20 MetaCore pathways enriched in the *AP1AR*-associated module, showing predominant enrichment of cell-cycle regulation, DNA replication, and DNA-damage checkpoint pathways (x-axis: –log10 p-value). **(B)** Representative MetaCore network illustrating *AP1AR*-related cell-cycle and DNA-replication programs, including regulation of the G1/S transition, chromatin remodeling, and MCM/CMG complex loading. **(C)** Bar plot of the top 20 MetaCore pathways enriched in the *AP1S3*-associated module, highlighting PLAU-mediated cell adhesion, cytoskeleton and ECM remodeling, apoptosis, and growth-factor signaling. **(D)** Representative MetaCore map depicting PLAU/uPAR–integrin–VEGFR/EGFR signaling and downstream cascades that regulate integrin-mediated cell adhesion, actin cytoskeleton remodeling, cell migration, and angiogenesis.
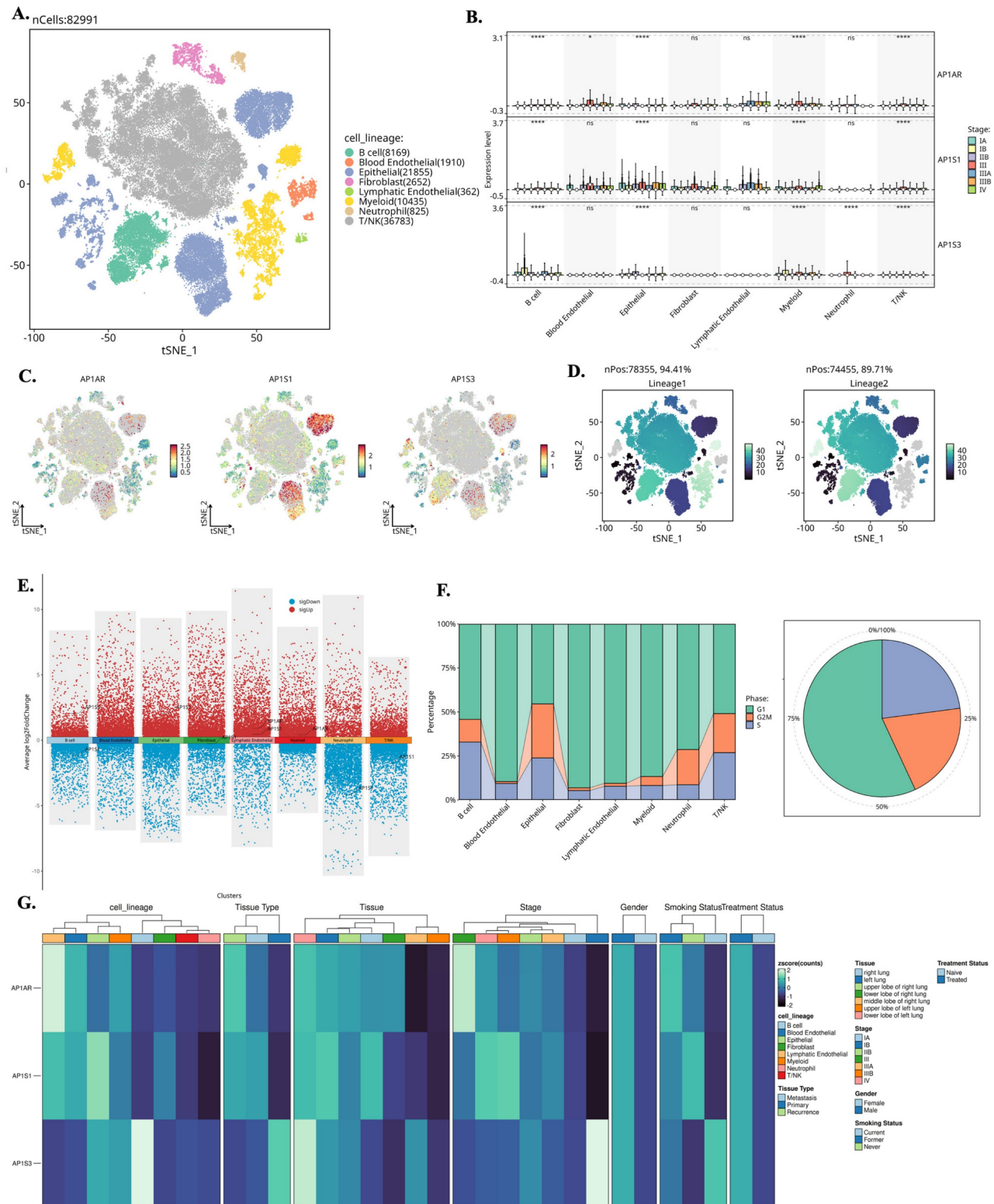
Figure 6. Single-cell transcriptomic landscape of *AP1AR*, *AP1S1*, and *AP1S3* in lung cancer. (A) t-SNE map of 82,991 cells from GSE202159 dataset, colored by major cell lineages. **(B)** Box plots showing normalized expression of *AP1AR*, *AP1S1*, and *AP1S3* across cell lineages and pathological stages, with highest expression in malignant epithelial and fibroblast cell types. **(C)** Feature plots of *AP1AR*, *AP1S1*, and *AP1S3* projected onto the t-SNE map, highlighting spatial localization of high-expressing clusters. **(D)** t-SNE maps illustrating lineage-level enrichment patterns (Lineage 1 and Lineage 2), indicating preferential accumulation of *AP1AR*-high cells within malignant epithelial subclusters. **(E)** Differential-expression analysis comparing *AP1AR*/*AP1S1*/*AP1S3*-high versus -low cells across lineages, shown as scatter plots of average log2 fold change; red and blue dots denote significantly upregulated and downregulated genes, respectively. **(F)** Cell-cycle phase distribution of each lineage (stacked bar plots) and of all cells combined (pie chart), indicating the proportions of cells in G1/M, G2/M, and S phases. **(G)** Heatmap of *AP1AR*, *AP1S1*, and *AP1S3* expression stratified by cell lineage, unsupervised cluster, tissue type (normal lung, primary tumor, recurrence), tumor stage, gender, smoking status, and treatment status, demonstrating consistent enrichment of *AP1AR* and *AP1S3* in more aggressive tumor subsets.
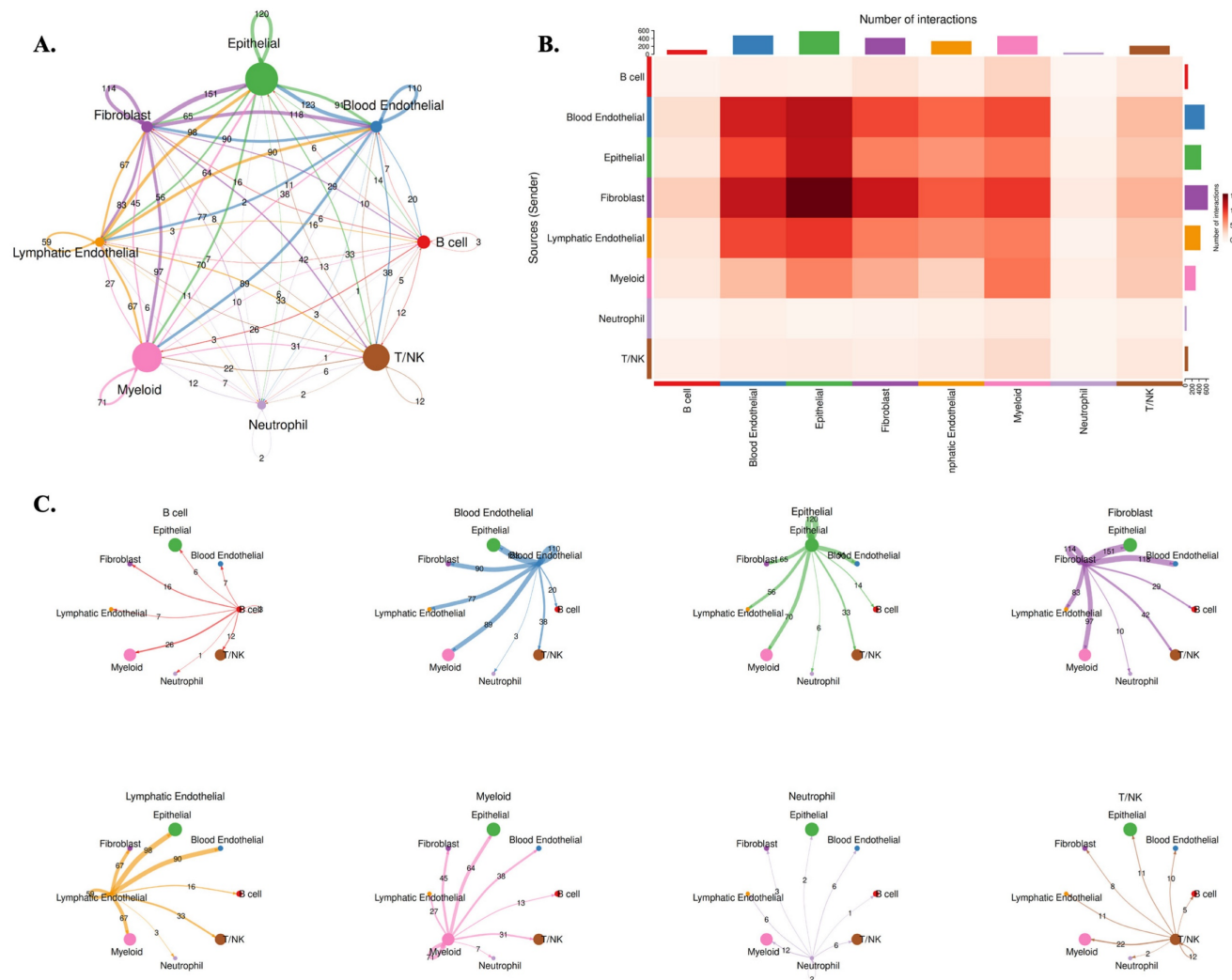
Figure 7. Cell–cell communication landscape in *AP1AR*-high lung tumors. (A) Global intercellular communication network inferred by CellChat for *AP1AR*-high samples. Nodes represent major cell lineages (B cell, blood endothelial, epithelial, fibroblast, lymphatic endothelial, myeloid, neutrophil, and T/NK), with node size proportional to the total number of incoming and outgoing interactions; edge thickness reflects the overall communication probability between lineages. **(B)** Heatmap summarizing the number of significant ligand–receptor interactions from sender (rows) to receiver (columns); darker colors indicate a higher interaction count, highlighting intensive crosstalk among epithelial, fibroblast, and endothelial cell types. **(C)** Directional network plots for each lineage, illustrating its outgoing communication to other cell types. Arrow width denotes interaction strength, revealing fibroblast-, epithelial-, and endothelial-centered signaling hubs in *AP1AR*-high lung tumors.

Our analyses further validated *AP1S3* as a clinically relevant adaptor gene, linking it to oncogenic signaling and immune-related pathways, while *AP1S1* showed associations with metabolic reprogramming and immune regulation. Cross-histotype analyses in LUSC confirmed that both *AP1AR* and *AP1S3* activate convergent EMT, PI3K/AKT/mTOR, and apoptosis pathways. Single-cell transcriptomics localized *AP1AR* and *AP1S3* primarily to malignant epithelial and fibroblast cell types, particularly in proliferative states, with pseudotime trajectories revealing progressive activation along EMT-like branches. At the mechanistic level, CellChat modeling indicated that *AP1AR*-high tumors exhibit a communication-intensive tumor microenvironment, with fibroblast and epithelial populations acting as signaling hubs for

immune and stromal interactions. Conversely, *AP1AR*-low tumors displayed diminished intercellular connectivity, particularly in fibroblast-to-epithelial and immune-to-tumor signaling, consistent with a dampened paracrine landscape. Functional enrichment analyses (GSEA, MetaCore) implicated *AP1AR* in cell-cycle progression, DNA replication checkpoints, hypoxia, and EMT, while *AP1S3* was linked to PI3K/AKT, KRAS, NF-κB, and MYC target pathways, connecting adaptor biology to both proliferation and immune modulation. Protein-level validation via IHC confirmed detectable *AP1AR* in tumor tissues, aligning with transcriptional and functional findings. CRISPR dependency screens indicated that *AP1AR* contributes to LUAD cell fitness, supporting a non-redundant role in tumor maintenance.

Pharmacogenomic analyses revealed that *AP1AR* upregulation correlates with resistance to chemotherapeutics and targeted inhibitors, whereas *AP1S1*, *AP1S3*, *AP1M2*, and *AP1B1* showed context-dependent associations with drug sensitivity. Network analyses placed *AP1AR* centrally within AP-1 adaptor-associated protein interaction space, consistent with curated protein-protein associations and enrichment data.

Overall, these converging multi-omics findings highlight *AP1AR* and *AP1S3* as the most clinically relevant AP-1 adaptors in lung cancer, elucidating their roles in proliferation, stress adaptation, immune modulation, and drug response. This framework provides a strong foundation for biomarker development and hypothesis-driven therapy selection, offering insights into the broader contributions of AP-1 adaptor biology to lung tumorigenesis and the tumor microenvironment. Our results further reinforced these findings of *AP1S3* by linking adaptor biology to oncogenic signaling and immune pathways, while *AP1S1* showed associations with metabolic reprogramming and immune regulation. The inclusion of LUSC GSEA results strengthened this conclusion, showing that both *AP1AR* and *AP1S3* activate convergent EMT, PI3K/AKT/mTOR, and apoptosis signatures across histological subtypes. Single-cell analyses underpinned these results by grounding them in the TME, revealing that *AP1AR* and *AP1S3* are preferentially expressed in malignant epithelial and fibroblast cell types, particularly during proliferative states. An additional pseudotime reconstruction demonstrated progressive activation of *AP1AR* along EMT-like trajectories, and the CellChat analysis revealed attenuated fibroblast-epithelial and immune-tumor signaling in *AP1AR*-low contexts, suggesting that adaptor regulation may influence both proliferation and intercellular communication. These inferences are consistent with the established roles of AP-1 adaptors in TGN-to-endosome trafficking and signaling homeostasis, and with CellChat's validated framework for network-level communication inference [81].

The most interesting finding is the involvement of *AP1AR* across multiple analytic layers. *AP1AR* expression was elevated in LUAD compared to normal tissues and demonstrated a strong association with OS. We additionally observed marked promoter hypomethylation in tumor samples, supporting an epigenetic mechanism for *AP1AR* activation. Unlike other AP-1 adaptor family members, *AP1AR* has not, to our knowledge, been functionally characterized in lung cancer; nevertheless, external resources document variable tumor protein detection, which

aligns with our IHC observations. CRISPR dependency screening confirmed that *AP1AR* moderately contributes to the fitness of lung-cancer cells, implying a non-redundant role in growth maintenance, and these interpretations are supported by the robustness and cross-study concordance of modern CRISPR dependency resources. GSEA and MetaCore analyses implicated *AP1AR* in cell-cycle progression, DNA-replication checkpoints, hypoxia, and EMT hallmark processes of tumor aggressiveness. Pseudotime trajectories further revealed that *AP1AR* expression peaks during G2/M and EMT-associated transitions, paralleling enrichment for DNA-repair gene signatures. Moreover, high *AP1AR* expression was correlated with resistance to chemotherapeutics and targeted agents, suggesting potential clinical implications for therapy stratification. CellChat modeling added a layer of interpretation, as *AP1AR*-low tumors exhibited globally reduced network connectivity, particularly between the stromal and epithelial cell types, consistent with a dampened paracrine signaling landscape. At the protein level, *AP1AR* was detectable by IHC, further validating its biological relevance. Single-cell analyses localized *AP1AR* to malignant epithelial clusters enriched in proliferative phases, providing strong evidence that it may act directly within tumor-driving cell types. Our analyses identified *AP1S3* as a second clinically relevant AP-1 adaptor gene in lung cancer. *AP1S3* was significantly upregulated in tumors and associated with poorer survival. Pathway analyses linked it to PI3K/AKT, KRAS, NF-κB-driven inflammatory responses, and MYC target activation, consistent with prior evidence that *AP1S3* modulates keratinocyte autophagy and enhances IL-36–dependent inflammatory signaling, connecting adaptor biology to immune pathways with potential oncogenic effects. *AP1S1* was also elevated, though with more modest survival associations; it regulates EGFR trafficking in NSCLC, and its perturbation promotes lysosomal EGFR degradation and alters TKI response, while literature links STAT3 activity to oxidative phosphorylation and therapy resistance, supporting an immune–metabolic interpretation [82, 83].

Other family members showed variable contributions. *AP1B1* and *AP1G1* participate in receptor trafficking, including EGFR polarity and recycling, and depletion of AP-1 or partners such as *GGA2* reduces EGFR surface levels and suppresses growth. AP-1 and *RAB12* cooperate in post-EGF trafficking steps that modulate downstream signaling outputs [84, 85]. *AP1M2* was enriched in apoptotic and hypoxia-related pathways, whereas *AP1S2* and *AP1M1* exhibited heterogeneous expression and

weaker survival associations. Pharmacogenomic analyses suggested that *AP1M2* and *AP1B1* sensitize cells to selected small-molecule inhibitors. Network analysis positioned *AP1AR* centrally within the AP-1 adaptor protein interaction network, consistent with curated protein–protein association and enrichment data. Overall, family-wide trends collectively highlight cell-cycle control, hypoxia responses, epithelial-to-mesenchymal transition, and tumor–stroma communication, providing a framework for biomarker development and hypothesis-driven therapy selection [86-88].

5. Conclusions

In conclusion, our integrated multi-omics and single-cell analyses identify *AP1AR* as the most consistent AP-1 adaptor signal in lung cancer, with the strongest evidence in adenocarcinoma. *AP1AR* shows transcriptional upregulation, independent associations with survival, promoter hypomethylation, enrichment of proliferation and epithelial to mesenchymal transition programs, and localization to tumor-driving cell types with altered stromal communication when low. These convergent layers nominate *AP1AR* as a clinically relevant biomarker and a candidate for translational prioritization, including hypothesis driven therapy stratification that will require prospective validation. Overall, the AP-1 adaptor complex emerges as an underexplored contributor to lung cancer biology. *AP1AR* stands out as a tractable focus for future mechanistic studies, biomarker development, and clinical evaluation aimed at therapy selection guided by adaptor gene expression.

Supplementary Material

Supplementary figures.
https://www.jcancer.org/v17p0142s1.pdf

Data availability statement

All datasets used in this study are publicly available. Supporting data can be obtained from the corresponding author upon reasonable request.

Competing Interests

The authors have declared that no competing interest exists.

References

1. Bray F, Ferlay J, Soerjomataram I, Siegel RL, Torre LA, Jemal A. Global cancer statistics 2018: GLOBOCAN estimates of incidence and mortality worldwide for 36 cancers in 185 countries. CA: A Cancer Journal for Clinicians. 2018; 68: 394-424.
2. Siegel RL, Miller KD, Wagle NS, Jemal A. Cancer statistics, 2023. CA Cancer J Clin. 2023; 73: 17-48.
3. Chen CL, Tseng PC, Chao YP, Shen TJ, Jhan MK, Wang YT, et al. Polypeptide antibiotic actinomycin D induces Mcl-1 uncanonical downregulation in lung cancer cell apoptosis. Life Sci. 2023; 321: 121615.
4. Tseng P-C, Chen C-L, Lee K-Y, Feng P-H, Wang Y-C, Satria RD, et al. Epithelial-to-mesenchymal transition hinders interferon-γ-dependent immunosurveillance in lung cancer cells. Cancer Letters. 2022; 539: 215712.
5. Wu SY, Chen CL, Tseng PC, Chiu CY, Lin YE, Lin CF. Fractionated ionizing radiation facilitates interferon-γ signaling and anticancer activity in lung adenocarcinoma cells. J Cell Physiol. 2019; 234: 16003-10.
6. Robinson MS. Adaptable adaptors for coated vesicles. Trends Cell Biol. 2004; 14: 167-74.
7. Salarolli RT, Alvarenga L, Cardozo L, Teixeira KTR, de SGML, Lima JD, et al. Can curcumin supplementation reduce plasma levels of gut-derived uremic toxins in hemodialysis patients? A pilot randomized, double-blind, controlled study. Int Urol Nephrol. 2021; 53: 1231-8.
8. Zatreanu D, Robinson HMR, Alkhatib O, Boursier M, Finch H, Geo L, et al. Polθ inhibitors elicit BRCA-gene synthetic lethality and target PARP inhibitor resistance. Nat Commun. 2021; 12: 3636.
9. Szymanski EA, Henriksen J. Reconfiguring the Challenge of Biological Complexity as a Resource for Biodesign. mSphere. 2022; 7: e0054722.
10. Feng F, Yu S, Wang Z, Wang J, Park J, Wilson G, et al. Non-pharmacological and pharmacological interventions relieve insomnia symptoms by modulating a shared network: A controlled longitudinal study. Neuroimage Clin. 2019; 22: 101745.
11. Jeong J, Hwang YE, Lee M, Keum S, Song S, Kim JW, et al. Downregulation of AP1S1 causes the lysosomal degradation of EGFR in non-small cell lung cancer. J Cell Physiol. 2023; 238: 2335-47.
12. Xiao D, Wang Q, Yan H, Lv X, Zhao Y, Zhou Z, et al. Adipose-derived stem cells-seeded bladder acellular matrix graft-silk fibroin enhances bladder reconstruction in a rat model. Oncotarget. 2017; 8: 86471-87.
13. Lin JC, Liu TP, Chen YB, Huang TS, Chen TY, Yang PM. Inhibition of CDK9 exhibits anticancer activity in hepatocellular carcinoma cells via targeting ribonucleotide reductase. Toxicol Appl Pharmacol. 2023; 471: 116568.
14. Lin JC, Liu TP, Chen YB, Yang PM. PF-429242 exhibits anticancer activity in hepatocellular carcinoma cells via FOXO1-dependent autophagic cell death and IGFBP1-dependent anti-survival signaling. Am J Cancer Res. 2023; 13: 4125-44.
15. Hsieh YY, Du JL, Yang PM. Repositioning VU-0365114 as a novel microtubule-destabilizing agent for treating cancer and overcoming drug resistance. Mol Oncol. 2024; 18: 386-414.
16. Hsieh YY, Cheng YW, Wei PL, Yang PM. Repurposing of ingenol mebutate for treating human colorectal cancer by targeting S100 calcium-binding protein A4 (S100A4). Toxicol Appl Pharmacol. 2022; 449: 116134.
17. Ko CC, Yang PM. Hypoxia-induced MIR31HG expression promotes partial EMT and basal-like phenotype in pancreatic ductal adenocarcinoma based on data mining and experimental analyses. J Transl Med. 2025; 23: 305.

18. Hoadley KA, Yau C, Hinoue T, Wolf DM, Lazar AJ, Drill E, et al. Cell-of-Origin Patterns Dominate the Molecular Classification of 10,000 Tumors from 33 Types of Cancer. Cell. 2018; 173: 291-304.e6.

19. Zhang JX, Wang L, Hou HY, Yue CL, Wang L, Li HJ. Age-related impairment of navigation and strategy in virtual star maze. BMC Geriatr. 2021; 21: 108.

20. Cao J, Spielmann M, Qiu X, Huang X, Ibrahim DM, Hill AJ, et al. The single-cell transcriptional landscape of mammalian organogenesis. Nature. 2019; 566: 496-502.

21. Chandrashekar DS, Bashel B, Balasubramanya SAH, Creighton CJ, Ponce-Rodriguez I, Chakravarthi B, et al. UALCAN: A Portal for Facilitating Tumor Subgroup Gene Expression and Survival Analyses. Neoplasia. 2017; 19: 649-58.

22. Comprehensive molecular profiling of lung adenocarcinoma. Nature. 2014; 511: 543-50.

23. Chiang YC, Wang CY, Kumar S, Hsieh CB, Chang KF, Ko CC, et al. Metal ion transporter SLC39A14-mediated ferroptosis and glycosylation modulate the tumor immune microenvironment: pan-cancer multi-omics exploration of therapeutic potential. Cancer Cell Int. 2025; 25: 363.

24. Su BH, Kumar S, Cheng LH, Chang WJ, Solomon DD, Ko CC, et al. Multi-omics profiling reveals PLEKHA6 as a modulator of β-catenin signaling and therapeutic vulnerability in lung adenocarcinoma. Am J Cancer Res. 2025; 15: 3106-27.

25. Xuan DTM, Yeh IJ, Liu HL, Su CY, Ko CC, Ta HDK, et al. A comparative analysis of Marburg virus-infected bat and human models from public high-throughput sequencing data. Int J Med Sci. 2025; 22: 1-16.

26. Dwivedi B, Mumme H, Satpathy S, Bhasin SS, Bhasin M. Survival Genie, a web platform for survival analysis across pediatric and adult cancers. Sci Rep. 2022; 12: 3069.

27. Tang Z, Kang B, Li C, Chen T, Zhang Z. GEPIA2: an enhanced web server for large-scale expression profiling and interactive analysis. Nucleic Acids Res. 2019; 47: W556-w60.

28. Győrffy B, Lanczky A, Eklund AC, Denkert C, Budczies J, Li Q, et al. An online survival analysis tool to rapidly assess the effect of 22,277 genes on breast cancer prognosis using microarray data of 1,809 patients. Breast Cancer Res Treat. 2010; 123: 725-31.

29. Kumar S, Wu CC, Wulandari FS, Chiao CC, Ko CC, Lin HY, et al. Integration of multi-omics and single-cell transcriptome reveals mitochondrial outer membrane protein-2 (MTX-2) as a prognostic biomarker and characterizes ubiquinone metabolism in lung adenocarcinoma. J Cancer. 2025; 16: 2401-20.

30. Xuan DTM, Wu CC, Wang WJ, Hsu HP, Ta HDK, Anuraga G, et al. Glutamine synthetase regulates the immune microenvironment and cancer development through the inflammatory pathway. Int J Med Sci. 2023; 20: 35-49.

31. Xuan DTM, Yeh IJ, Su CY, Liu HL, Ta HDK, Anuraga G, et al. Prognostic and Immune Infiltration Value of Proteasome Assembly Chaperone (PSMG) Family Genes in Lung Adenocarcinoma. Int J Med Sci. 2023; 20: 87-101.

32. Goldman M, Craft B, Hastie M, Repečka K, McDade F, Kamath A, et al. The UCSC Xena platform for public and private cancer genomics data visualization and interpretation. biorxiv. 2018: 326470.

33. Arafeh R, Shibue T, Dempster JM, Hahn WC, Vazquez F. The present and future of the Cancer Dependency Map. Nature Reviews Cancer. 2025; 25: 59-73.

34. Uhlén M, Fagerberg L, Hallström BM, Lindskog C, Oksvold P, Mardinoglu A, et al. Proteomics. Tissue-based map of the human proteome. Science. 2015; 347: 1260419.

35. Chiao CC, Liu YH, Phan NN, An Ton NT, Ta HDK, Anuraga G, et al. Prognostic and Genomic Analysis of Proteasome 20S Subunit Alpha (PSMA) Family Members in Breast Cancer. Diagnostics (Basel). 2021; 11.

36. Anuraga G, Wang WJ, Phan NN, An Ton NT, Ta HDK, Berenice Prayugo F, et al. Potential Prognostic Biomarkers of NIMA (Never in Mitosis, Gene A)-Related Kinase (NEK) Family Members in Breast Cancer. J Pers Med. 2021; 11.

37. Ta HDK, Wang WJ, Phan NN, An Ton NT, Anuraga G, Ku SC, et al. Potential Therapeutic and Prognostic Values of LSM Family Genes in Breast Cancer. Cancers (Basel). 2021; 13.

38. Liu CJ, Hu FF, Xie GY, Miao YR, Li XW, Zeng Y, et al. GSCA: an integrated platform for gene set cancer analysis at genomic, pharmacogenomic and immunogenomic levels. Brief Bioinform. 2023; 24.

39. Rees MG, Seashore-Ludlow B, Cheah JH, Adams DJ, Price EV, Gill S, et al. Correlating chemical sensitivity and basal gene expression reveals mechanism of action. Nat Chem Biol. 2016; 12: 109-16.

40. Iorio F, Knijnenburg TA, Vis DJ, Bignell GR, Menden MP, Schubert M, et al. A Landscape of Pharmacogenomic Interactions in Cancer. Cell. 2016; 166: 740-54.

41. Wu YJ, Chiao CC, Chuang PK, Hsieh CB, Ko CY, Ko CC, et al. Comprehensive analysis of bulk and single-cell RNA sequencing data reveals Schlafen-5 (SLFN5) as a novel prognosis and immunity. Int J Med Sci. 2024; 21: 2348-64.

42. Anuraga G, Lang J, Xuan DTM, Ta HDK, Jiang JZ, Sun Z, et al. Integrated bioinformatics approaches to investigate alterations in transcriptomic profiles of monkeypox infected human cell line model. J Infect Public Health. 2024; 17: 60-9.

43. Wang CY, Xuan DTM, Ye PH, Li CY, Anuraga G, Ta HDK, et al. Synergistic suppressive effects on triple-negative breast cancer by the combination of JTC-801 and sodium oxamate. Am J Cancer Res. 2023; 13: 4661-77.

44. Korotkevich G, Sukhov V, Sergushichev A. Fast gene set enrichment analysis. bioRxiv. 2019: 060012.

45. Liberzon A, Birger C, Thorvaldsdóttir H, Ghandi M, Mesirov JP, Tamayo P. The Molecular Signatures Database (MSigDB) hallmark gene set collection. Cell Syst. 2015; 1: 417-25.

46. Wang CY, Chao YJ, Chen YL, Wang TW, Phan NN, Hsu HP, et al. Upregulation of peroxisome proliferator-activated receptor-α and the lipid metabolism pathway promotes carcinogenesis of ampullary cancer. Int J Med Sci. 2021; 18: 256-69.

47. Liu HL, Yeh IJ, Phan NN, Wu YH, Yen MC, Hung JH, et al. Gene signatures of SARS-CoV/SARS-CoV-2-infected ferret lungs in short- and long-term models. Infect Genet Evol. 2020; 85: 104438.

48. Wu YH, Yeh IJ, Phan NN, Yen MC, Hung JH, Chiao CC, et al. Gene signatures and potential therapeutic targets of Middle East respiratory syndrome coronavirus (MERS-CoV)-infected human lung adenocarcinoma epithelial cells. J Microbiol Immunol Infect. 2021; 54: 845-57.

49. Szklarczyk D, Kirsch R, Koutrouli M, Nastou K, Mehryary F, Hachilif R, et al. The STRING database in 2023: protein-protein association networks and functional enrichment analyses for any sequenced genome of interest. Nucleic Acids Res. 2023; 51: D638-d46.

50. Glasner A, Rose SA, Sharma R, Gudjonson H, Chu T, Green JA, et al. Conserved transcriptional connectivity of regulatory T cells in the tumor microenvironment informs new combination cancer therapy strategies. Nat Immunol. 2023; 24: 1020-35.

51. Megill C, Martin B, Weaver C, Bell S, Prins L, Badajoz S, et al. cellxgene: a performant, scalable exploration platform for high dimensional sparse matrices. bioRxiv. 2021: 2021.04.05.438318.

52. Solomon DD, Ko CC, Chen HY, Kumar S, Wulandari FS, Xuan DTM, et al. A machine learning framework using urinary biomarkers for pancreatic ductal adenocarcinoma prediction with post hoc validation via single-cell transcriptomics. Brief Bioinform. 2025; 26.

53. Li CY, Anuraga G, Chang CP, Weng TY, Hsu HP, Ta HDK, et al. Repurposing nitric oxide donating drugs in cancer therapy through immune modulation. J Exp Clin Cancer Res. 2023; 42: 22.

54. Hagerling C, Gonzalez H, Salari K, Wang CY, Lin C, Robles I, et al. Immune effector monocyte-neutrophil cooperation induced by the primary tumor prevents metastatic progression of breast cancer. Proc Natl Acad Sci U S A. 2019; 116: 21704-14.

55. Lee KT, Chen DP, Loh ZJ, Chung WP, Wang CY, Chen PS, et al. Benign polymorphisms in the BRCA genes with linkage disequilibrium is associated with cancer characteristics. Cancer Sci. 2024; 115: 3973-85.

56. Chen HK, Chen YL, Wang CY, Chung WP, Fang JH, Lai MD, et al. ABCB1 Regulates Immune Genes in Breast Cancer. Breast Cancer (Dove Med Press). 2023; 15: 801-11.

57. Chen YL, Lee KT, Wang CY, Shen CH, Chen SC, Chung WP, et al. Low expression of cytosolic NOTCH1 predicts poor prognosis of breast cancer patients. Am J Cancer Res. 2022; 12: 2084-101.

58. Ye PH, Li CY, Cheng HY, Anuraga G, Wang CY, Chen FW, et al. A novel combination therapy of arginine deiminase and an arginase inhibitor targeting arginine metabolism in the tumor and immune microenvironment. Am J Cancer Res. 2023; 13: 1952-69.

59. Jin S, Guerrero-Juarez CF, Zhang L, Chang I, Ramos R, Kuan CH, et al. Inference and analysis of cell-cell communication using CellChat. Nat Commun. 2021; 12: 1088.

60. Mwale PF, Hsieh CT, Yen TL, Jan JS, Taliyan R, Yang CH, et al. Chitinase-3-like-1: a multifaceted player in neuroinflammation and degenerative pathologies with therapeutic implications. Mol Neurodegener. 2025; 20: 7.

61. Chen IC, Lin HY, Liu ZY, Cheng WJ, Yeh TY, Yang WB, et al. Repurposing Linezolid in Conjunction with Histone Deacetylase Inhibitor Access in the Realm of Glioblastoma Therapies. J Med Chem. 2025; 68: 2779-803.

62. Shen CJ, Chen HC, Lin CL, Thakur A, Onuku R, Chen IC, et al. Contribution of Prostaglandin E2-Induced Neuronal Excitation to Drug Resistance in Glioblastoma Countered by a Novel Blood-Brain Barrier Crossing Celecoxib Derivative. Adv Sci (Weinh). 2025: e06336.

63. Chen HC, Lin HY, Chiang YH, Yang WB, Wang CH, Yang PY, et al. Progesterone boosts abiraterone-driven target and NK cell therapies against glioblastoma. J Exp Clin Cancer Res. 2024; 43: 218.

64. Liu CC, Yang WB, Chien CH, Wu CL, Chuang JY, Chen PY, et al. CXCR7 activation evokes the anti-PD-L1 antibody against glioblastoma by remodeling CXCL12-mediated immunity. Cell Death Dis. 2024; 15: 434.

65. Cassiano GC, Martinelli A, Mottin M, Neves BJ, Andrade CH, Ferreira PE, et al. Whole genome sequencing identifies novel mutations in malaria parasites resistant to artesunate (ATN) and to ATN + mefloquine combination. Front Cell Infect Microbiol. 2024; 14: 1353057.

66. Kwee I, Martinelli A, Khayal LA, Akhmedov M. metaLINCS: an R package for meta-level analysis of LINCS L1000 drug signatures using stratified connectivity mapping. Bioinform Adv. 2022; 2: vbac064.

67. Maseng MJ, Tawe L, Thami PK, Seatla KK, Moyo S, Martinelli A, et al. Association of CYP2B6 Genetic Variation with Efavirenz and Nevirapine Drug Resistance in HIV-1 Patients from Botswana. Pharmgenomics Pers Med. 2021; 14: 335-47.

68. Wickham H. ggplot2. Wiley interdisciplinary reviews: computational statistics. 2011; 3: 180-5.

69. Xuan DTM, Wu CC, Kao TJ, Ta HDK, Anuraga G, Andriani V, et al. Prognostic and immune infiltration signatures of proteasome 26S subunit, non-ATPase

(PSMD) family genes in breast cancer patients. Aging (Albany NY). 2021; 13: 24882-913.

70. Choy TK, Wang CY, Phan NN, Khoa Ta HD, Anuraga G, Liu YH, et al. Identification of Dipeptidyl Peptidase (DPP) Family Genes in Clinical Breast Cancer Patients via an Integrated Bioinformatics Approach. Diagnostics (Basel). 2021; 11.

71. Hinton PR, McMurray I, Brownlow C. SPSS explained: Routledge; 2014.

72. Akhmedov M, Martinelli A, Geiger R, Kwee I. Omics Playground: a comprehensive self-service platform for visualization, analytics and exploration of Big Omics Data. NAR Genom Bioinform. 2020; 2: lqz019.

73. Tang D, Chen M, Huang X, Zhang G, Zeng L, Zhang G, et al. SRplot: A free online platform for data visualization and graphing. PLoS One. 2023; 18: e0294236.

74. Wickham H, Sievert C. ggplot2: elegant graphics for data analysis: Springer, New York; 2009.

75. Chen PS, Hsu HP, Phan NN, Yen MC, Chen FW, Liu YW, et al. CCDC167 as a potential therapeutic target and regulator of cell cycle-related networks in breast cancer. Aging (Albany NY). 2021; 13: 4157-81.

76. Doyle SR, Tracey A, Laing R, Holroyd N, Bartley D, Bazant W, et al. Genomic and transcriptomic variation defines the chromosome-scale assembly of Haemonchus contortus, a model gastrointestinal worm. Commun Biol. 2020; 3: 656.

77. Marks ND, Winter AD, Gu HY, Maitland K, Gillan V, Ambroz M, et al. Profiling microRNAs through development of the parasitic nematode Haemonchus identifies nematode-specific miRNAs that suppress larval development. Sci Rep. 2019; 9: 17594.

78. Lin JC, Liu TP, Yang PM. CDKN2A-Inactivated Pancreatic Ductal Adenocarcinoma Exhibits Therapeutic Sensitivity to Paclitaxel: A Bioinformatics Study. J Clin Med. 2020; 9.

79. Liu LW, Hsieh YY, Yang PM. Bioinformatics Data Mining Repurposes the JAK2 (Janus Kinase 2) Inhibitor Fedratinib for Treating Pancreatic Ductal Adenocarcinoma by Reversing the KRAS (Kirsten Rat Sarcoma 2 Viral Oncogene Homolog)-Driven Gene Signature. J Pers Med. 2020; 10.

80. Hsieh YY, Liu TP, Chou CJ, Chen HY, Lee KH, Yang PM. Integration of Bioinformatics Resources Reveals the Therapeutic Benefits of Gemcitabine and Cell Cycle Intervention in SMAD4-Deleted Pancreatic Ductal Adenocarcinoma. Genes (Basel). 2019; 10.

81. Robinson MS, Antrobus R, Sanger A, Davies AK, Gershlick DC. The role of the AP-1 adaptor complex in outgoing and incoming membrane traffic. J Cell Biol. 2024; 223.

82. Hu Y, Dong Z, Liu K. Unraveling the complexity of STAT3 in cancer: molecular understanding and drug discovery. Journal of Experimental & Clinical Cancer Research. 2024; 43: 23.

83. Yang L, Ying S, Hu S, Zhao X, Li M, Chen M, et al. EGFR TKIs impair lysosome-dependent degradation of SQSTM1 to compromise the effectiveness in lung cancer. Signal transduction and targeted therapy. 2019; 4: 25.

84. Uemura T, Suzuki T, Dohmae N, Waguri S. Clathrin adapters AP-1 and GGA2 support expression of epidermal growth factor receptor for cell growth. Oncogenesis. 2021; 10: 80.

85. Cotton CU, Hobert ME, Ryan S, Carlin CR. Basolateral EGF receptor sorting regulated by functionally distinct mechanisms in renal epithelial cells. Traffic. 2013; 14: 337-54.

86. Pacini C, Duncan E, Gonçalves E, Gilbert J, Bhosle S, Horswell S, et al. A comprehensive clinically informed map of dependencies in cancer cells and framework for target prioritization. Cancer Cell. 2024; 42: 301-16.e9.

87. Wu F, Yang J, Liu J, Wang Y, Mu J, Zeng Q, et al. Signaling pathways in cancer-associated fibroblasts and targeted therapy for cancer. Signal Transduction and Targeted Therapy. 2021; 6: 218.

88. Asmerian H, Alberts J, Sanetra AM, Diaz AJ, Silm K. Role of adaptor protein complexes in generating functionally distinct synaptic vesicle pools. J Physiol. 2025; 603: 5889-901.